

# Friction stir welding (FSW) casting aluminium alloys with wrought alloys

## Introduction

The FSW process is a welding method used in joining aluminium alloys, including casting aluminium alloys and wrought alloys, which are particularly difficult to weld using other methods.

This study presents selected results of tests of butt welding casting aluminium alloys as well as casting aluminium alloys welded with wrought alloys. Such arrangements of materials can be joined by means of the FSW method offering high quality of joints. Joining such alloys can be conducted using tools made of conventional tool steels. Their sufficient durability guarantees high repeatability of the welding process [1].

## Materials tested

The tests of a welding process and of the quality of joints were carried out for the following aluminium alloys: casting aluminium alloy EN AC-43200 (AK9) and wrought aluminium alloy EN AW-2017A (PA6). EN AC-43200 alloy may be joined by means of other welding methods, e.g. arc welding, whereas

EN AW-2017A alloy is difficult to weld by arc methods [2, 3]. The chemical composition of the materials tested is presented in Table 1.

## Testing station and process parameters

In order to build up joints of casting aluminium alloys EN AC-43200 it was necessary to apply a triflute-type tool with special notches on the probe facilitating the motion of plastic material around the probe. In turn, to produce joints made of casting aluminium alloy EN AC-43200 welded with wrought aluminium alloy EN AW-2017A it was necessary to apply a conventional tool equipped with a probe in the form of a threaded roller. The tools were made of tungsten and molybdenum high-speed steel (HS-6-5-2).

The tests involved the use of 6mm-thick plates which were pressed against each other and immobilized by means of special holders on the welding machine. Next, they were butt welded without cleaning the surface of the interface. Plates made of casting aluminium alloy were welded at the tool rotational

Table 1. Chemical composition of aluminium alloys used in tests [4, 5]

No.	Alloy designation		Element content, %								
	Numerical	Chemical symbols	Si	Cu	Mg	Mn	Fe	Zn	Zn	Ni	Al
1.	EN AC-43200 (AK9)	EN AC-AlSi10Mg(Cu)	10	≤0.35	0.33	≤0.55	≤0.65	≤0.20	≤0.35	≤0.15	rest
2.	EN AW-2017A (PA6)	EN AW-Al Cu4MgSi(A)	≤0.8	≤4.50	≤1.00	≤1.00	0.70	-	0.25	-	rest

Mgr inż. Damian Miara, dr inż. Adam Pietras – Instytut Spawalnictwa, Zakład Technologii Zgrzewania i Inżynierii Środowiska /Department of Resistance and Friction Welding and Environmental Engineering/

speed  $V_n = 500, 700, 900$  and  $1300$  rev./min and at the linear welding rate  $V_z = 200$  mm/min. Plates made of EN AC-43200 and EN AW-2017A alloys were welded at the tool rotational speed  $V_n = 560, 710$  and  $900$  rev./min as well as at the linear welding rate  $V_z 112, 180$  and  $280$  mm/min.

In order to weld the plates made of casting aluminium alloy EN AC-43200 it was necessary to use a welding machine for FSW, made on the base of a numerically controlled milling machine FNE 50NC, manufactured by AVIA S.A. (Figure 1a). Welding of plates made of casting aluminium alloy EN AC-43200 with wrought alloy EN AW-2017A was performed using a FSW welding machine, built on the base of a conventional milling machine of FYF32JU2 type, manufactured by JAFO S.A.

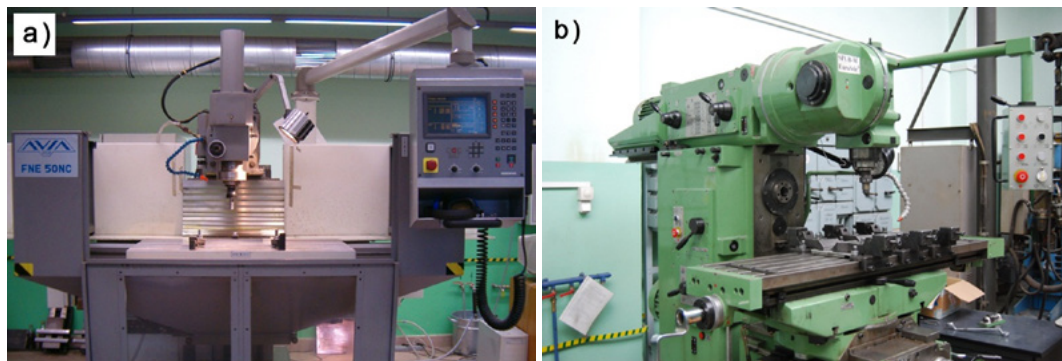


Fig. 1. FSW welding stations: a) numerically controlled milling machine AVIA FNE 50NC; b) vertical conventional milling machine FYF32JU2

## Quality examination of the joints made of casting aluminium alloy EN AC-43200

### *Non-destructive testing of joints*

At the initial stage of the tests of casting aluminium alloy EN AC-43200 it was necessary to determine the linear welding rate at which the face of the weld was formed properly and the forces and moments of welding did not exceed the capacity of the friction welding machine (for the tested range of the rotational speed of welding). Such joints made in the selected range of welding parameters were subject to visual inspection.

The process progressed in a stable manner in the selected range of welding, without visible irregularities of the surface and without the material sticking to the tool.

The examination revealed that the joints had a correct structure of the face of the weld with a slight impression of the shoulder, without visible discontinuities and excessive deformation of the material. On the side of the root of the weld there was no trace of the former interface line. The surface of the weld root was smooth and continuous, without any sign of discontinuities. The view of the selected joints made of casting aluminium alloy EN AC-43200 seen from the face of the weld is presented in Figure 2.

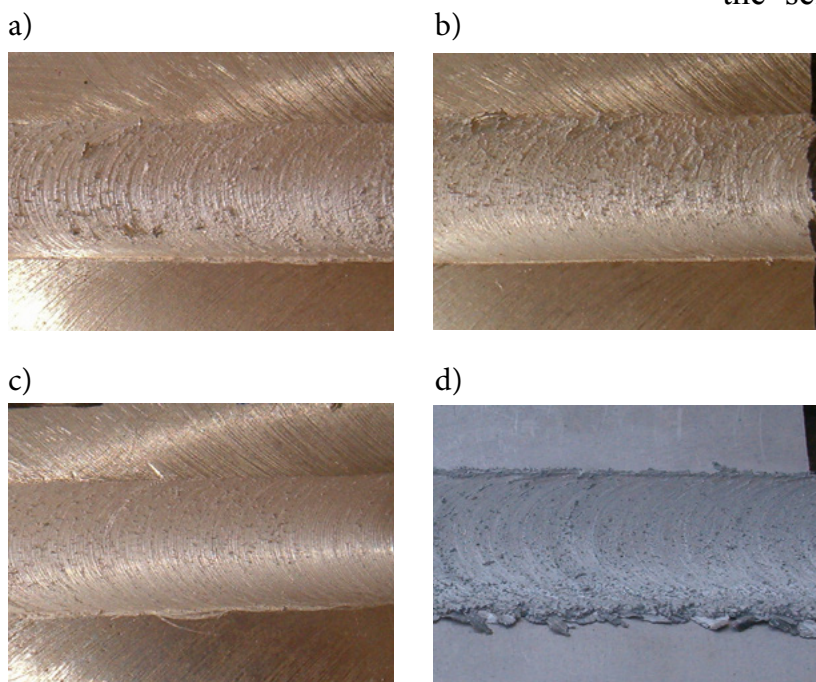


Fig. 2. View of the joints made of casting aluminium alloy EN AC-43200. Welding parameters:  $V_n$  [rev./min] /  $V_z$  [mm/min]: a) 500/200, b) 700/200, c) 900/200, d) 1300/200,

Radiographic examination of the joints made of aluminium alloy EN AC-43200, carried out using a Seifert Eresco-made 200HF device, did not show any imperfections or discontinuities in the properly executed welds, within the range of the selected welding parameters. All the joints were characterized by full metal continuity along the weld axis.

A typical radiogram of a properly built weld made of casting aluminium alloy EN AC-43200 is presented in Figure 3.



Fig. 3. Radiogram of the joint made of casting aluminium alloy EN AC-43200. Welding parameters:  
 $V_n = 1300 \text{ rev./min}$ ,  $V_z = 200 \text{ mm/min}$

### ***Strength tests of thermo-mechanically deformed weld material***

Due to the fact that casting aluminium alloy is a brittle material, the samples subjected to tensile tests (in compliance with the standard [6]) cracked in the clamps of the testing machine or outside the weld; the dispersion of tensile forces was significant. Therefore, in order to determine the strength properties of the thermo-mechanically plasticised material, it was necessary to cut out 12 mm-wide samples of material along the weld axis (Figure 4). Next, the samples were subjected to tensile tests until breaking on an INSTRON 4210 testing machine.

Table 2. Tensile strength of the fragments of thermo-mechanically deformed weld material (for the welds made of casting aluminium alloy EN AC-43200)

No.	Tool	Welding parameters		Average tensile strength $R_m$ [MPa]
		$V_n$ [rev./min]	$V_z$ [mm/min]	
1	T Ø8 (5.8) Ø22	500	200	133.2
2	T Ø8 (5.8) Ø22	700	200	141.8
3	T Ø8 (5.8) Ø22	900	200	145.6
4	T Ø8 (5.8) Ø22	1300	200	131.1

Note: average measured tensile strength of parent metal of alloy EN AC-43200 : 105.2 MPa

The results of tensile tests of the fragments of the thermo-mechanically deformed weld material are presented in Table 2. For comparison purposes the table also contains the average value of tensile strength of the parent metal.

The results of tensile tests indicate that, as regards casting aluminium alloys EN AC-43200, the average strength of thermo-mechanically deformed weld material is higher by approximately 20% - 30% than the tensile strength of the parent metal. The elongation during the tensile test ranged from 4 mm to 12 mm.

The analysis of the results of strength-related tests of the weld material deformed thermo-mechanically during welding proves that the strength depends on the rotational speed of the tool (Table 2). Initially, the tensile strength of the thermo-mechanically de-

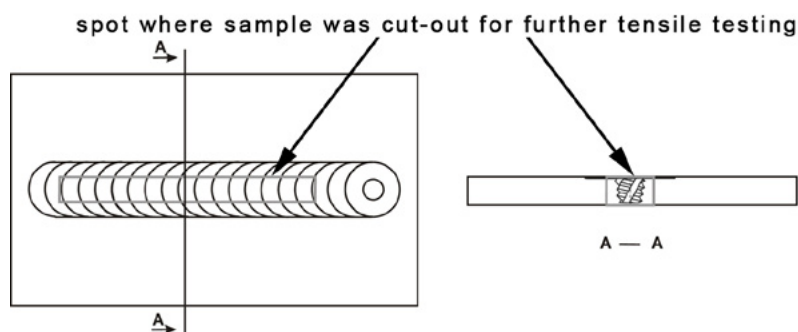


Fig. 4. Method of sample preparation (cut-out) for strength tests: samples were cut out along the weld axis - fragment of the thermo-mechanically deformed weld material



formed weld material increases, along with an increasing tool rotational speed up to 900 rev./min, and after exceeding this value begins to decrease. At low rotational speeds the tool does not heat the welding area sufficiently and, as a result, it is not possible to obtain a properly built up weld. At high rotational speeds the tool excessively heats the weld with the shoulder on the weld face side, at the same time insufficiently plasticising the weld inside. In addition, the shoulder “pushes” excessively plasticised material from the welding surface outside the welding area.

### Structure of welds

Metallographic tests of the welds were conducted by means of an optical microscope MeF4M manufactured by LEICA and with a scanning microscope Philips M525. The tests involved the analysis of the central area of the weld (the so-called weld nugget), the area deformed thermo-mechanically, and the heat affected zone. Etching was carried out using Keller’s etchant.

Depending on linear welding rate it is possible to see the impact of the shoulder and the probe of the tool on the heating of material and the formation of a weld. In each case (at a tool rotational speed of 500 rev./min) one can easily observe the impact of the heat generated from the side of the shoulder, plasticising the material around the rotating tool (Fig. 5). The weld takes a trapezoid shape. At a high rotational speed (1300 rev./min) the weld takes the shape of concentrically arranged circles, forming the so-called weld nugget (Fig. 6). At high rotational speeds the impact of the shoulder is minimum and the probe of the tool has a decisive influence on the heating and stirring of the weld material.

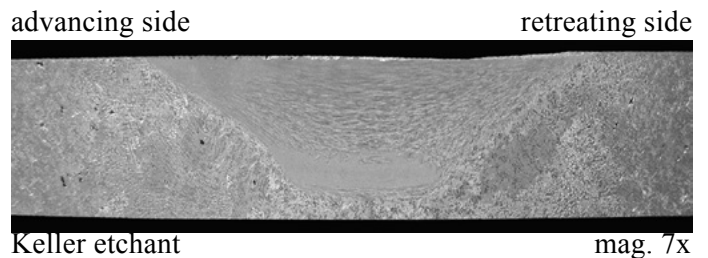


Fig. 5. Macrostructure of the FSW weld made of casting aluminium alloy EN AC-43200. Welding parameters:  $V_n = 500$  rev./min,  $V_z = 200$  mm/min

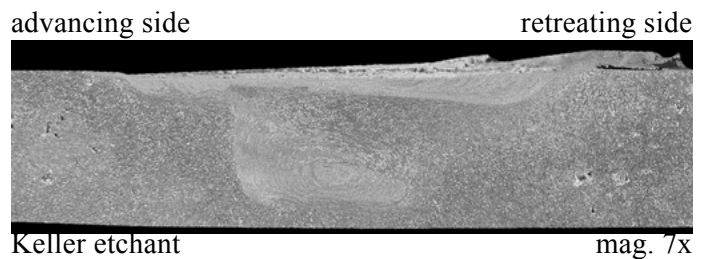


Fig. 6. Macrostructure of the FSW weld made of casting aluminium alloy EN AC-43200. Welding parameters:  $V_n = 1300$  rev./min,  $V_z = 200$  mm/min

### Weld hardness measurements

Vickers hardness tests involved the parent metal, weld area and the heat affected zone. The places of measurements are marked in the drawings. The results of hardness measurements reveal a course typical of friction stir welded joints – an increase in the central areas of the weld (weld nugget) and reduced hardness in the heat affected zone. It was also possible to observe greater differences in hardness on the retreating side than on the advancing side. An exemplary course of hardness of FSW sample is presented in Figure 7.

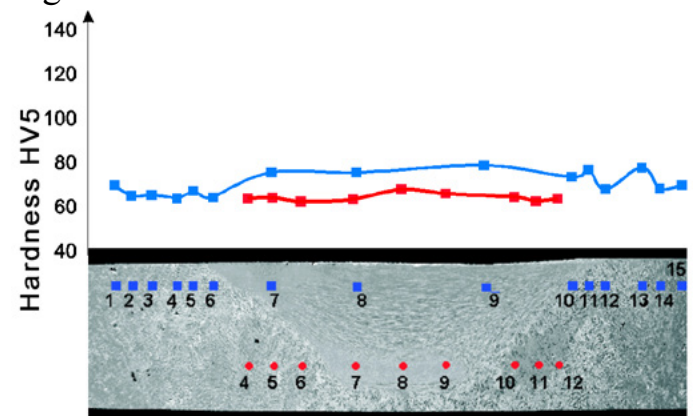


Fig. 7. Structure of the weld and hardness in sections of friction stir welded joint made of alloy EN AC-43200. Welding parameters:  $V_n = 500$  rev./min,  $V_z = 200$  mm/min

## Tests of quality of joints of casting aluminium alloy EN AC-43200 welded with wrought aluminium alloy EN AW-2017A

### *Non-destructive tests of joints*

During initial welding attempts it was possible to observe that the compact structure of a weld can be obtained only when casting aluminium alloy EN AC-43200 is laid on the retreating side and wrought aluminium alloy EN AW-2017A is laid on the advancing side. During the tests it was also possible to notice that the type of tool has no greater impact on the quality of produced welds. For this reason the process of welding was carried out using a tool which was simpler and easier to make i.e. a conventional tool. The quality of welds was evaluated on the basis of the course of the welding process and the manner in which the face and the root of the weld were formed. The results of visual inspection (in the form of a view of joints) are presented in Figure 8.

The visual inspection of butt welded joints made of casting aluminium alloy EN AC-43200 and wrought aluminium alloy EN AW-2017A reveal the shape of the face and

the root of the weld typical of a FSW process. Depending on a tool's rotational speed and linear welding rate, the external view of the joints varies only slightly – welds take regular shapes. On the face side of these welds it was not possible to observe any imperfection of the “no joint” type. On the root side it was not possible to observe any traces related to the contact of joined materials (no visible notches), which indicates a proper course of a welding process carried out with a tool of an appropriate length of the probe.

### *Measurement of forces and torque*

During welding, force and torque values were measured by means of a LOWSTIR measurement device, provided with special software. The device makes it possible to monitor a welding process and record courses of welding parameters intended for further analysis. The table below presents average values of forces and torque affecting materials being welded during welding in a stabilised state (Table 3). An exemplary graph of the course of forces and torque during welding is presented in Figure 9.

The values of the force in the direction of welding, pressure force, and torque vary depending on welding process parameters. The values of the force in the direction of welding range from 1.04 to 1.88 kN (forces increase along with an increasing rotational speed of the tool). The pressure force ranges from 11.04 to 18.12 kN (forces increase along with an increasing rotational speed of the tool). In turn, an increasing rotational speed is

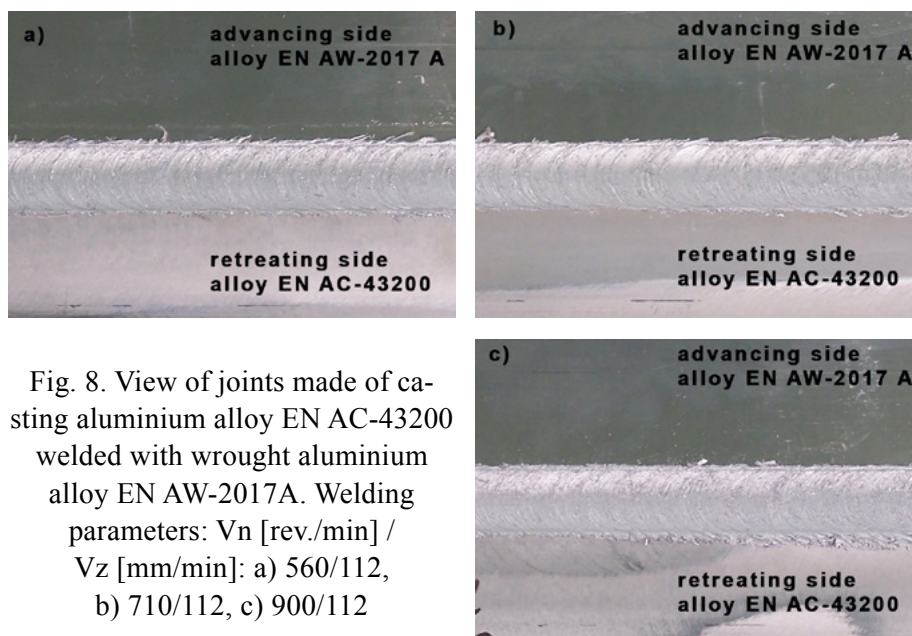


Fig. 8. View of joints made of casting aluminium alloy EN AC-43200 welded with wrought aluminium alloy EN AW-2017A. Welding parameters:  $V_n$  [rev./min] /  $V_z$  [mm/min]: a) 560/112, b) 710/112, c) 900/112

Table 3. Values of forces and moment recorded during welding of plates made of aluminium alloys EN AC-43200 (on the retreating side) and EN AW-2017A (on the advancing side)

No.	Welding parameters		Force in direction of welding [kN]	Welding pressure force [kN]	Torque [Nm]
	Vn [rev./min]	Vz [mm/min.]			
1.	560	112	1,04	11,04	34,81
2.	560	180	1,34	12,95	34,92
3.	560	280	1,46	13,56	35,57
4.	710	112	1,29	13,28	26,09
5.	710	180	1,43	13,55	26,81
6.	710	280	1,58	15,83	28,89
7.	900	112	1,42	15,23	17,64
8.	900	180	1,52	18,12	20,63
9.	900	280	1,88	17,90	20,97

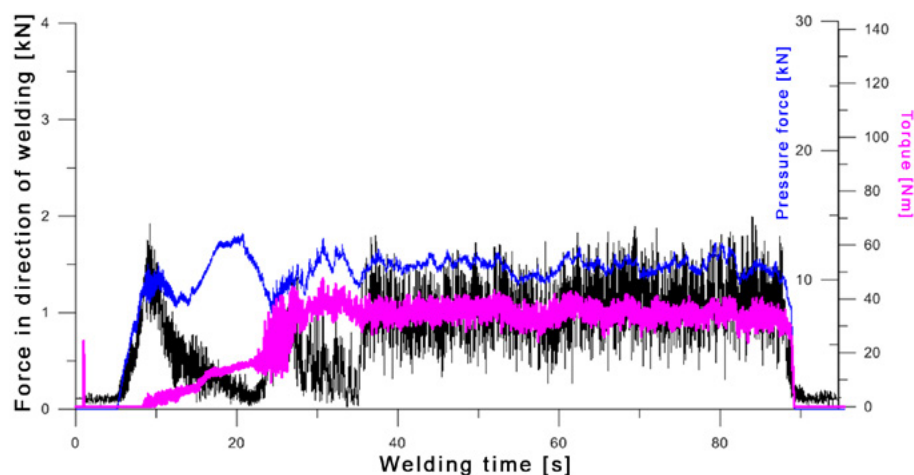


Fig. 9. Course of force in the direction of welding, pressure force and torque, recorded during welding of plates made of aluminium alloys EN AC-43200 and EN AW-2017A. Welding parameters: Vn=560 rev./min, Vz=112 mm/min

Table 4. Results of temperature measurement on the surface of faces of welds built up with a conventional tool

No.	Welding parameters		Temperature on the surface of the face of weld (in weld axis) T [°C]
	Vn [rev./min]	Vz [mm/min]	
1.	560	112	360
2.	560	180	244
3.	560	280	308
4.	710	112	382
5.	710	180	387
6.	710	280	361
7.	900	112	403
8.	900	180	411
9.	900	280	402

accompanied by a slightly decreasing torque ranging from 17.64 to 35,57 Nm. An increasing linear welding rate (at a constant rotational speed of the tool) is accompanied by increasing values of forces and torque, yet their growth is very low.

### **Measurements of welding area temperature**

During welding, the temperature of the upper surface of the welding area was measured for all process parameters; the measurements were carried out by thermographic camera VIGOCAM v50. Selected results of welding area temperature measurements using the thermographic camera are presented in Table 4.

Along with an increasing rotational speed of the tool, the maximum temperature on the surface of the face of the weld rises slightly. The value of the temperature depends on the amount of material “thrown out” by the welding tool outside the welding area. The smaller the volume of the flash, the higher the temperature, which results from flash being heated faster. In turn, along with an increasing linear welding rate the average temperature on the surface of the weld face decreases slightly. The results of welding area temperature measurements reveal that the temperatures on the retreating side are slightly higher than those on the advancing side.



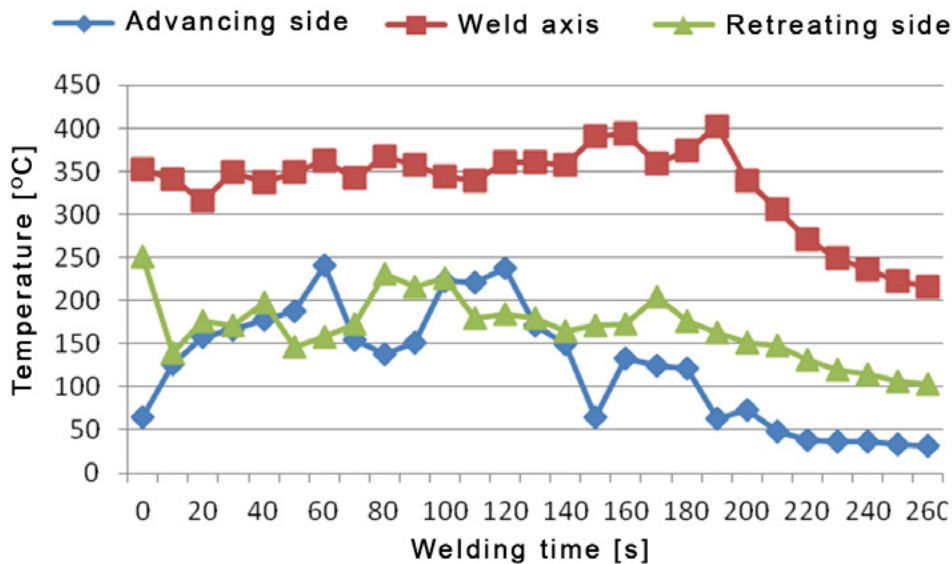


Fig. 10. Course of temperature in the function of welding time in various areas of a welded joint. Welding parameters:  $V_n=560$  rev./min,  $V_z=112$  mm/min

Figure 10 presents a typical course of temperature in the function of welding time for three measurement points (in the weld axis and 25mm away from the axis – on the retreating side and on the advancing side).

### Structure of welds

The process of welding of EN AC-43200 alloy with EN AW-2017A alloy was stable; the weld was characterised by proper structure for relatively low values of linear welding rate e.g. 112 mm/min. The figure below presents a typical structure of an FSW weld made of casting aluminium alloy welded with wrought aluminium alloy (Fig. 11).

In the weld made of EN AW-2017A alloy (on the advancing side) and EN AC-43200 (on the retreating side) it was possible to observe small precipitates of aluminium phases



Fig. 11. Macrostructure of FSW weld made of EN AW- 2017A (on the advancing side) and EN AC-43200 (on the retreating side) alloys, built up with a conventional tool. Welding parameters:  $V_n=560$  rev./min,  $V_z=112$  mm/min

– silicon and aluminium – copper (Fig. 12). The precipitates were present with various intensities in the whole of the deformation area and the heat affected zone.

Strongly magnified images of the structure of the weld made of the casting alloy welded with the wrought alloy revealed the presence of small structural discontinuities.

The discontinuities were present mainly in the interface of individual layers of the weld, at the terminal area of the impact of the tool pin (Fig. 13) and on the

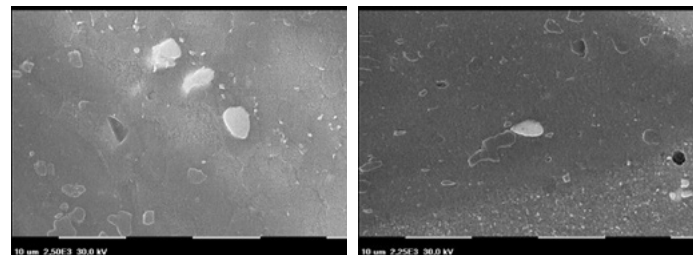


Fig. 12. Brittle precipitates in weld area of EN AW-2017A and EN AC-43200: AlSi (dark) and AlCu (bright): a) area of retreating b) central area of the weld

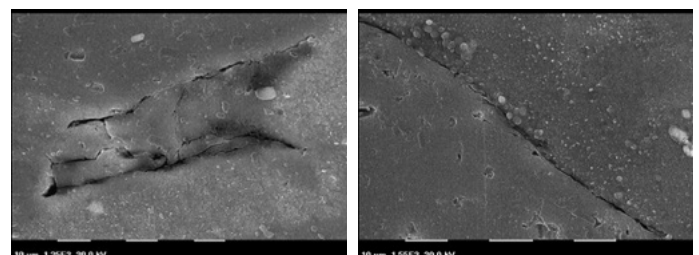


Fig. 13. Discontinuity of material in the weld: a) near root of the weld, b) in the interface of parent metal (on the left) and layer deformed thermo-mechanically (on the right)

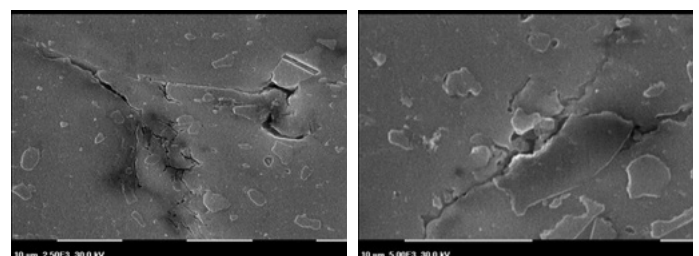


Fig. 14. Cracks on the boundary of brittle precipitates AlSi in weld material of EN AW-2017A and EN AC-43200; the lower part of the weld with impact of the end of the tool pin

brittle precipitates of phases, expanding from these discontinuities (Fig. 14). The reason for the presence of these discontinuities also lay in the difference of stresses accompanying the welding process.

The presence of the discontinuities entails a pursuit of optimum welding conditions such as the lowest possible temperature in the weld area.

### Generation of heat and supply of energy

During a welding process heat can be generated as a result of friction of tool surface against materials being welded and as a result of deformation of material around the tool [7]. The calculation of the heat source power at a given moment of friction is possible if one assumes that phenomena occurring during FSW are the same as in the process of friction welding (phenomena taking place between the tool and the surface of materials being welded). On this basis the power of the heat source on the surface of the tool–material interface can be calculated from the following basic dependence (knowing the torque and rotational speed of the tool):

$$N_{cQ} = Mt \times 2\pi \times \omega \quad (1)$$

where:

$N_{cQ}$  – heat source power [W],

$Mt$  - torque [Nm],

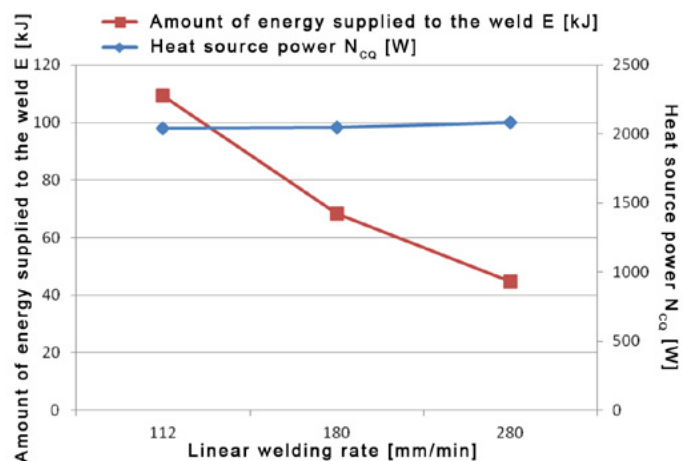


Fig. 15. Dependence of energy supplied to the weld and of heat source power on linear welding rate (at  $V_n = 560$  rev./min)

$\omega$  – rotational speed of the tool [rev./s].

In addition, knowing the time needed to build up the weld and using dependence (2) it was possible to calculate the total amount of energy supplied to the weld. The results of calculations of heat source power generated at a given moment and of the total amount of energy supplied to the weld are presented in Table 5.

$$E = N_{cQ} \times t \quad (2)$$

where:

$E$  – amount of energy supplied to the weld [kJ],

$t$  – welding time [s].

The comparison of the total amount of energy supplied to the weld and of heat source power depending on linear welding rate is presented in Figure 15.

Table 5. Total energy supplied to the weld on a stabilised section of the weld

No.	Rotational speed of the tool $V_n$ [rev./min]	Welding rate $v$ [m/s]	Welding time in stabilised state of the weld $t$ [s]	Heat source power $N_{cQ}$ [W]	Total energy $E$ [kJ]
1.	560	0.0019	53.57	2040.3	109.30
2.	560	0.0030	33.33	2046.8	68.23
3.	560	0.0047	21.43	2084.9	44.68
4.	710	0.0019	53.57	1938.8	103.87
5.	710	0.0030	33.33	1992.3	66.41
6.	710	0.0047	21.43	2146.9	46.01
7.	900	0,0019	53,57	1661,7	89,02
8.	900	0,0030	33,33	1943,3	64,78
9.	900	0,0047	21,43	1975,4	42,33



Along with an increase in linear welding rate one can observe a slight increase in heat power source and a decrease in energy supplied to the weld (on its stabilised section). In turn, an increase in the rotational speed of the tool is accompanied by a decrease both in the heat source power and the total amount of energy supplied to the weld. Depending on welding process parameters the heat source power is between approximately 1660 W and 2140 W, whereas the total amount of energy supplied to the weld ranges from approximately 42 kJ to 109 kJ.

## Summary

The tests of welding of casting alloys, conducted at a specified welding rate but at various values of rotational speed of the tool, revealed that the proper quality of joints, from the point of view of weld strength and structure, can be obtained within a relatively vast range of process parameters. An increase in rotational speed results in changes of weld structure. When rotational speeds are low the process of welding and plasticising of material in the welding area is mainly affected by shoulder and the weld takes trapezoid shape. During welding at high rotational speeds it is possible to observe the area of intense stirring in the central area of the weld i.e. the so-called weld nugget. [8].

The strength tests of the thermo-mechanically deformed material cut out of the weld revealed that, for EN AC-43200 alloy, the tensile strength of the weld material is higher than of the parent metal. Elongation during the tensile test was  $4 \div 12$  mm.

Hardness measurements of joints revealed a distribution typical for friction stir welded joints – a slight hardness increase in the central areas of the weld (weld nugget) and a hardness decrease in the heat affected zone.

The test revealed that casting aluminium alloys are properly weldable by means of the FSW method within a limited range of welding parameters. Proper joint quality can be obtained by maintaining the basic conditions of a properly conducted welding process.

In the case of joining casting aluminium alloys with wrought alloys it was possible to obtain proper quality using a relatively low linear welding rate, similarly as in publication [9]. In addition, obtaining welds of compact structure is possible only with wrought aluminium alloy EN AW-2017A laid on the advancing side, and casting aluminium alloy EN AC-43200 laid on the retreating side.

A change in welding process parameters (tool rotational speed and linear welding rate) is accompanied by a slight change in temperature distribution on the surface of the face of the weld. An increase in the tool rotational speed causes a slight increase in the average maximum temperature on the surface of the weld face. An increase in linear welding rate causes a decrease in the average temperature on the surface of the weld face. The temperature on the surface of the weld face is also connected with the size of the flash generated during a welding process.

The knowledge of the registered moment of friction made it possible to calculate heat source power and the total amount of energy supplied to the weld. An increase in linear welding rate is accompanied by an increase in heat source power, yet the total amount of energy supplied to the weld decreases.

The macro- and microscopic tests revealed proper structure of welds made of EN AW-2017A + EN AC-43200 alloys, yet strongly magnified images revealed the presence of small structural discontinuities (Fig. 12). It was ascertained that these

discontinuities were related to non-uniform heating and deformation of individual areas of material (Fig. 13a – at the terminal area affected by the tool pin, Fig. 13b – in the interface of individual layers of the weld) and that their propagation proceeded in the places of grouping of AlSi precipitates (Fig. 14). Micro-cracks which expanded around these precipitates were formed in built-up joints in the whole tested range of welding process parameters. In some cases micro-cracks were very few. In general, the presence of micro-cracks does not affect the strength of the whole joint, yet, in some cases may have an effect on its functional properties.

## Conclusions

1. Butt FSW technology can be applied for joining elements made of casting aluminium alloys.

2. FSW has a thermo-mechanical effect on a material in the welding area and increases its plasticity. The thermo-mechanically deformed material of the weld (for casting aluminium alloy EN AC-43200) is characterised by higher plasticity and tensile strength than the parent metal.

3. An increase in the rotational speed of the tool is accompanied by a decrease in the impact of shoulder on the shape and structure of the weld.

4. Adjusting proper parameters of a FSW process guarantees high quality of joints as well as compact and repeatable structure of welds obtained during the joining of casting alloys characterised by the same structure or alloys differing in chemical composition and physical properties.

5. The FSW process makes it possible to join casting alloys with wrought alloys. The properties of joints depend on the conditions in which a welding process is conducted and

the situation of alloys to be welded. Wrought alloys should be laid on the advancing side.

6. An increase in linear welding rate is accompanied by a slight increase in heat source power and by a decrease in the total amount of energy supplied to the weld.

## References

[1]. Cornell R., Bhadeshia H.K.D.H.: Aluminium-Silicon Casting Alloys, Cambridge, 2002.

[2]. Tokarski M.: Metaloznawstwo metali i stopów nieżelaznych w zarysie. Wydawnictwo Śląsk, Katowice 1994.

[3]. Pod red. J. Pilarczyka: Poradnik Inżyniera, Spawalnictwo, T. 2, WNT, Warszawa, 2007.

[4]. PN-EN 1706:2010. Aluminium i stopy aluminium - Odlewy - Skład chemiczny i własności mechaniczne.

[5]. PN-EN 573-3:2010. Aluminium i stopy aluminium - Skład chemiczny i rodzaje wyrobów przerobionych plastycznie - Część 3: Skład chemiczny i rodzaje wyrobów.

[6]. PN-EN ISO 6892-1:2010. Metale - Próba rozciągania - Część 1: Metoda badania w temperaturze pokojowej.

[7]. Chao Y., Tang W.: Heat Transfer in Friction Stir Welding – Experimental and numerical studies. Transactions of the ASME, 2003, nr 125.

[8]. Kim Y.G., Fujii H., Tsumura T., Komazaki T., Nakata K.: Effect of welding parameters on microstructure in the stir zone of FSW joints of aluminum die casting alloy. Materials Letters, 2006, vol. 60, nr 29-30.

[9]. Cavaliere P., A. Santis A., Panella F., Squillace A.: Effect of welding parameters on mechanical and microstructural properties of dissimilar AA6082–AA2024 joints produced by friction stir welding. Materials and Design, 2009, nr 30, str. 609–616.